

## Rod-like Polyelectrolyte Brushes with Mono- and Multivalent Counterions

H. FAZLI<sup>1</sup>, R. GOLESTANIAN<sup>1</sup>, P.L. HANSEN<sup>2</sup>, and M.R. KOLAHCHI<sup>1</sup>

<sup>1</sup> *Institute for Advanced Studies in Basic Sciences, Zanjan 45195-1159, Iran*

<sup>2</sup> *MEMPHYS-Center for Biomembrane Physics, Physics Department, University of Southern Denmark, DK-5230 Odense M, Denmark*

PACS 82.35.Rs – Polyelectrolytes

PACS 83.80.Xz – Liquid crystals: nematic, cholesteric, smectic, discotic, etc.

PACS 87.68.+z – Biomaterials and biological interfaces

**Abstract.** - A model of rod-like polyelectrolyte brushes in the presence of monovalent and multivalent counterions but with no added-salt is studied using Monte Carlo simulation. The average height of the brush, the histogram of rod conformations, and the counterion density profile are obtained for different values of the grafting density of the charge-neutral wall. For a domain of grafting densities, the brush height is found to be relatively insensitive to the density due to a competition between counterion condensation and inter-rod repulsion. In this regime, multivalent counterions collapse the brush in the form of linked clusters. Nematic order emerges at high grafting densities, resulting in an abrupt increase of the brush height.

---

Electrostatic correlation effects of highly charged macro-ions in aqueous solutions have recently attracted much attention [1]. Novel phenomena such as charge inversion and like-charge attraction, which cannot be understood within the Poisson-Boltzmann theory, appear to play a key role in biological processes such as DNA packaging [2] and cell scaffolding dynamics [3]. Such correlations, and their role in determining the overall structural properties of the system, are most pronounced in high density polyelectrolyte solutions where the charge “patterns” that form due to the correlations strongly interact with each other. If the polyelectrolyte is sufficiently stiff in its backbone structure [such as DNA and filamentous actin (F-actin)], a geometric constraint is imposed on the charges in each polyelectrolyte segment to adopt a more or less linear configuration, which makes a solution of such rod-like polyelectrolytes a patterned matrix for the counterions (that is, the ions of opposite charge that are present to neutralize the overall solution). The interplay between these correlations and patterns can lead to novel structural and dynamical properties [4–7], the study of which could be useful in understanding the biological phenomena mentioned above as well as designing functional biomimetic materials.

A common realization of such high density assemblies occurs in polyelectrolyte brushes [8], where charged polymers are end-grafted to surfaces. While polyelectrolyte brushes have been mostly studied because of their role in stabilization of colloidal suspensions, understanding their structural properties could help us in a variety of problems in biophysics and -technology. A case in point is filamentous microtubules, *i.e.* rod-like structures build from tubulin monomers with charged C-terminal amino-acid tails extending from the filament core [9]. The C-terminal tails seem to play key roles in microtubule function, e.g. in connection with binding of microtubule-associated proteins and processivity of the molecular

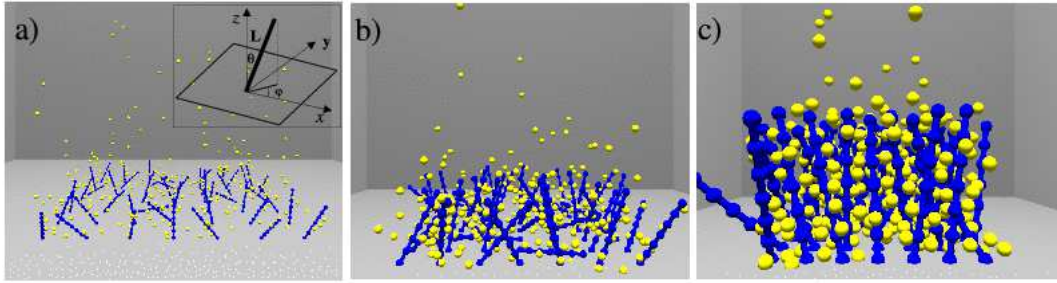


Fig. 1: Snapshots of the system with monovalent counterions: a)  $a = 1.2L$ , b)  $a = 0.55L$  and c)  $a = 0.25L$ . Inset: the schematic configuration of a polyelectrolyte rod of length  $L$  and two rotational degrees of freedom  $\theta$  and  $\phi$ .

motors that move along microtubules [10]. Presumably they form disordered brushes making it difficult to study them by systematic scattering and osmotic stress experiments [11]. Design of more effective DNA chips [12] may also benefit from a better understanding of rod-like polyelectrolyte brushes. Interestingly, STM studies suggest that densely grafted arrays of short single-stranded DNA molecules on gold substrates self-organize into disordered structures, and it takes an applied electric field normal to the grafting surface to align these brushes [13].

Most theoretical studies of polyelectrolyte brushes have focused on flexible chains, i.e. charged polymers that are longer than their persistence lengths. If the polyelectrolytes are sufficiently short or highly charged, they would behave effectively as charged rods [14] that are constrained to be very close to each other because of the brush structure; a feature that can bring about frustration [7]. Here, we study the structural properties of rodlike polyelectrolyte brushes in the presence of monovalent and trivalent counterions using Monte Carlo (MC) simulation techniques. We calculate the average thickness of the brush, the density profile of the counterions, and the statistics of the conformation of the rods, as functions of the surface coverage density. We find three distinct regimes for the collective behavior of the rods: (i) a weakly interacting regime at low densities where the counterions are dispersed in the solution (see Fig. 1a), (ii) an intermediate regime where the counterions are condensed in the brush (see Fig. 1b), and (iii) a novel nematic regime at high densities (see Fig. 1c). The counterion density profile is found to be depleted near the wall in the intermediate regime, while the statistics of the rod conformations show that a small fraction of the rods choose to lie on the surface as a result of electrostatic frustration. We also find that trivalent counterions collapse the brush in the intermediate regime by forming links between clusters of neighboring rods (see Fig. 2a). Interestingly, the height of the brush in the intermediate regime seems to depend very weakly on the areal density of the rods, both for monovalent and trivalent counterions.

We model each polyelectrolyte as a rigid rod of length  $L$  with  $N_m$  charged hard sphere monomers of diameter  $\sigma$  and charge  $q_m = -e$  distributed along it in a uniform periodic array.  $N_r$  polyelectrolytes are end grafted on a square lattice with a lattice constant  $a$  on a surface, so that the areal grafting density is  $\rho_a = 1/a^2$ . Each polyelectrolyte has two rotational degrees of freedom  $\theta$  and  $\phi$  (Fig. 1a). The counterions are modeled as hard-core spheres of diameter  $\sigma$  and they carry a charge  $q_c = Ze$  in which  $Z$  is the valence of the counterions. The system is electrostatically neutralized:  $N_c \times Z = N_r \times N_m$ , where  $N_c$  is the number of counterions.

We use Lekner summation method [15] to account for long-range Coulomb interactions by applying lateral periodic boundary conditions in  $x$  and  $y$  directions (see Fig. 1a), and the simulation box is finite in  $z$  direction, normal to the brush surface. Elementary moves for counterions, are chosen at random in the simulation box around it. For the polyelectrolyte

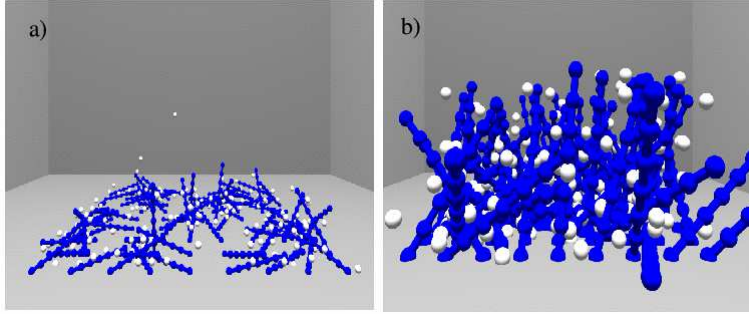


Fig. 2: Snapshots of the system with trivalent counterions at a)  $a = 0.65L$  and b)  $a = 0.25L$ .

rods the non-grafted end of each rod moves randomly on the surface of a hemisphere of radius  $L$ . For highly charged rods it is known that algorithms involving independent moves for the polyelectrolytes become inefficient since many counterions are linked to polyelectrolytes, and moving a rod away from these counterions would cost a lot of energy that effectively prohibits any Monte Carlo move [16]. To solve this problem, we follow Ref. [16] and look for all counterions at distances less than  $d$  of each rod and rotate them all together with the polyelectrolyte. Considering the acceptance rate of the MC moves, the value of  $d$  has been optimized to  $d = 2\sigma$ . We equilibrate the system by starting from different initial configurations and reaching the same stationary value of the Coulomb energy. In simulations with monovalent counterions, the equilibrium was reached after  $2 \times 10^4$  MC steps per particle for the smallest value of the lattice constant. For the case of trivalent counterions the equilibration time is  $3 \times 10^4$  MC steps per particle. The simulation box height in  $z$  direction,  $H$ , has been chosen in such a way that the results are independent of its value;  $H = 12L$  for monovalent and  $H = 8L$  for trivalent counterions.

To quantify the strength of the electrostatic energy relative to the thermal energy, we can define the Bjerrum length  $l_B = \frac{e^2}{\epsilon k_B T}$ , where  $\epsilon$  is the dielectric constant of the solvent. In our simulations, we chose to fix the Bjerrum length—which in room temperature is about 0.7 nm for water—to a fraction of the length of the rod, namely,  $l_B = L/7$ . This means that the length of rods is chosen to be about  $L \simeq 5$  nm at room temperature. We also fixed the diameter of the rods to  $\sigma = 0.1L$ . In the case of monovalent counterions, the simulation parameters were:  $N_m = 7$ ,  $N_r = 7 \times 7 = 49$ , and  $N_c = 343$ . Thermal averages were obtained over  $6 \times 10^4$  MC steps, after equilibrating the system. In simulations with trivalent counterions ( $Z = 3$ ), we chose:  $N_m = 7$ ,  $N_r = 9 \times 9 = 81$ , and  $N_c = 189$ , and thermal averages are calculated over  $9 \times 10^4$  MC steps after equilibration. Note that the Manning parameter  $\xi = \frac{ZN_m l_B}{L}$  [17] was set to  $\xi_1 = 1$  for monovalent, and  $\xi_3 = 3$  for trivalent counterions.

We vary the lattice constant  $a$ , keeping the other parameters fixed, and calculate the brush height as  $h = \frac{L}{N_r} \sum_{i=1}^{N_r} \langle \cos \theta_i \rangle$ , where  $\langle \dots \rangle$  denotes ensemble average. For each value of  $a$ , we start the system from a random initial configuration and calculate thermal averages after equilibration of the system. Figure 3 shows the brush height as a function of the lattice constant  $a$  for  $Z = 1$ . When the lattice constant is very large, the effective attraction of the rods to the counterions becomes very weak and the counterions evaporate away from them, while the long distance between the rods makes their own electrostatic interaction negligible. In this regime,  $\cos \theta$  has a uniform distribution with the thermal average of  $\frac{1}{2}$ , and the brush height is  $h = L/2$ . As the spacing  $a$  is reduced, the rods start to interact with each other electrostatically and the brush is swollen, as can be seen in Fig. 3. Note that in this regime the majority of the counterions are still away from the surface (see the snapshot of the system in Fig. 1a). To justify this observation, one can roughly consider the  $z = 0$  plane as a charged surface with the uniform charge density  $\sigma_s = \frac{N_m}{a^2}$ , for which it is

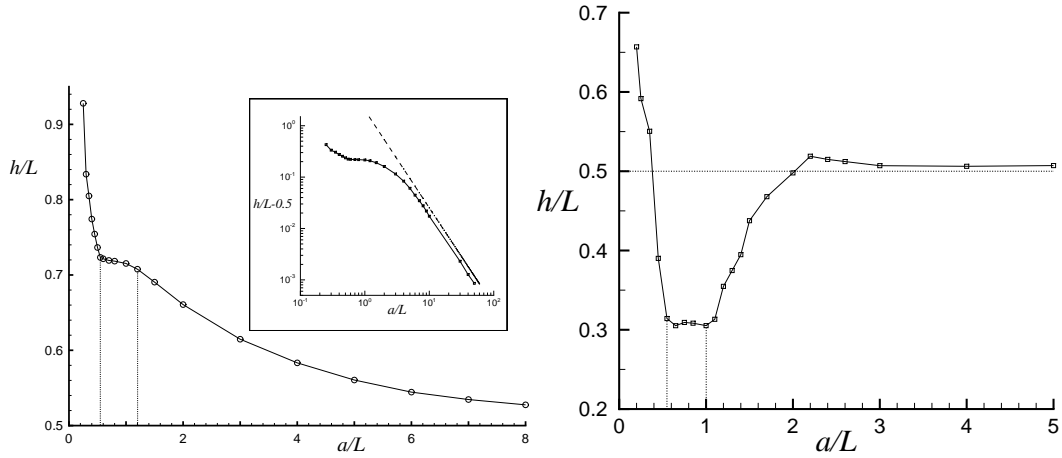


Fig. 3

Fig. 4

Fig. 3: The brush height as a function of the lattice constant  $a$ , in the presence of monovalent counterions. Inset: the log-log plot of  $h/L - 0.5$  as a function of  $a$  for  $Z = 1$ . At large lattice constants the brush height scales as  $a^{-2}$  (the dashed line has the slope of  $-2$ ).

Fig. 4: The brush height versus  $a$  in the presence of trivalent counterions.

known from Poisson-Boltzmann theory that the counterions are confined within a distance of  $\lambda = \frac{1}{2\pi Z l_B \sigma_s} = \frac{a^2}{2\pi Z l_B N_m}$ , called the Gouy-Chapman length. We can readily see that  $\lambda \gg L$ , so long as  $a \gg L$  and  $\lambda \gg a$  that is a requirement for the smeared surface charge density approximation to be justified.

The swelling of the brush in this regime seems to obey a scaling law of the form  $\frac{h}{L} - \frac{1}{2} \sim \frac{1}{a^2}$ , as demonstrated in the inset of Fig. 3. This scaling behavior can be understood by assuming that individual rods are fluctuating as dipoles in the presence of a uniform electric field as obtained from the smeared charge density  $\sigma_s$ , namely, the sum of monopole-dipole interactions which are the dominant terms in the multipole expansion valid for large  $a$ . The scaling behavior is reminiscent of that of flexible polyelectrolyte brushes in the Pincus regime [8].

Upon decreasing the lattice constant, the effective surface charge density of the brush is increased so that the counterions are attracted to the brush, as the snapshot of the system in Fig. 1b shows. This trend continues until a new regime sets in where all the counterions are confined within the brush, which is analogous to the osmotic regime in flexible polyelectrolyte brushes [8]. One could roughly estimate the onset of this crossover by setting the thickness of the counterion layer ( $\sim \lambda$ ) equal to the height of the brush ( $\sim L$ ), which yields  $a_{\times} \sim \xi^{1/2} L$ . In this regime, the counterions are involved in heavily screening the interaction between the rods, and thus one expects that the swelling slows down, as can be seen in the plateau-like feature in Fig. 3 for the intermediate range of  $0.55L < a < 1.2L$ . At higher densities, the rods are completely neutralized by the counterions, and the remaining excluded volume interaction among them promotes a novel nematic ordering that sets in sharply at  $a = 0.55L$  (see Fig. 3), similar to the Onsager nematic transition in 3D solutions of hard rods [18]. A typical snapshot of the system in the nematic phase is shown in Fig. 1c.

The picture becomes more complicated with the introduction of multivalent counterions. Figure 4 shows the brush height as a function of the lattice constant in the presence of trivalent counterions. For infinitely large  $a$  the brush height is still  $h = L/2$ , and it does swell initially as  $a$  is decreased similar to the monovalent case. However, once a sufficient fraction of the trivalent counterions are attracted to the rods and fluctuate in the vicinity of them, they give rise to a fluctuation-induced attraction [19]. This attractive interaction

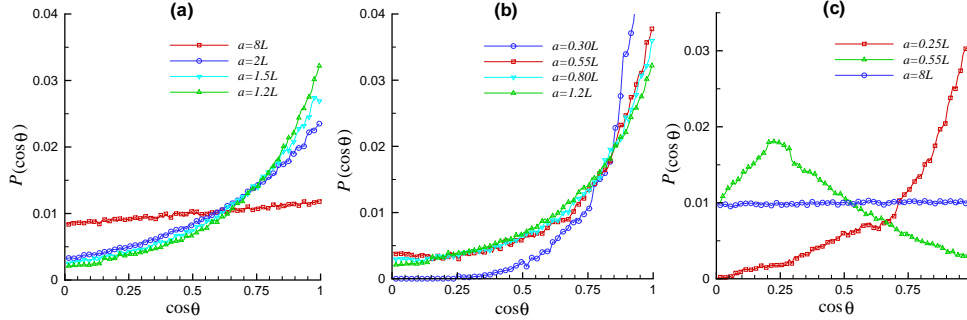


Fig. 5: The histogram of  $\cos \theta$  for a)  $Z = 1$  and  $a \geq 1.2L$ , b)  $Z = 1$  and  $a \leq 1.2L$ , and c)  $Z = 3$ .

competes with the repulsion between the rods and the result of this competition turns back the swelling of the brush around  $a = 2.2L$  (see Fig. 4). This trend becomes more drastic as of  $a = 2.0L$ , where the brush height is  $h = 0.5L$  again, because the trivalent counterions can now link the polyelectrolyte rods to each other (see Fig. 2a) and collapse the brush [20]. Similar to the monovalent case, an interesting plateau regime appears for  $0.55L < a < 1.0L$ , where the enhancement in the repulsion between the rods as  $a$  decreases is exactly balanced by the increased possibility of forming links between neighboring rods. This leads to the clusters growing in size more and more until at  $a = 0.55L$  the collection of now fully neutralized hard rods undergo a nematic transition; the brush height suddenly increases (see Fig. 4) and the rods become predominantly parallel, as the snapshot in Fig. 2b shows. Note that the onset of the nematic transition coincides in the two cases of mono- and trivalent counterions, in line with the suggestion that the transition is entirely driven by the excluded volume interaction.

In addition to the average thickness of the brush, it is instructive to monitor the histogram of the rod conformations  $P(\cos \theta)$  in the different regimes. In Fig. 5a,  $P(\cos \theta)$  is shown for four different lattice constants in the  $a \geq 1.2L$  domain, for monovalent case. We find that in this regime by decreasing  $a$ , the  $\cos \theta = 0$  part of the histogram decreases and the  $\cos \theta = 1$  part increases, which corresponds to a “normal” swelling of the brush. (At sufficiently large lattice constants the histogram shows a uniform distribution of  $\cos \theta$ , as expected.) As the lattice spacing is further reduced to  $a \leq 1.2L$ , the situation becomes more subtle, as Fig. 5b shows. For  $0.55L < a < 1.2L$  the trend of change in the  $\cos \theta = 0$  part of the histogram is different from Fig. 5a: decreasing the lattice constant  $a$  increases both the  $\cos \theta = 0$  and  $\cos \theta = 1$  parts of the histogram, while the intermediate region of the histogram decreases to maintain the normalization of the distribution. In this regime, the system presumably tries to lower the electrostatic repulsion between the polyelectrolytes by increasing angles between the neighboring rods and consequently some of the rods lie on the surface, as can be seen in the snapshot for  $a = 0.55L$  in Fig. 1b. For  $a < 0.55L$ , a drastic change of behavior is observed and the  $\cos \theta = 0$  part of the histogram vanishes, which signals the nematic ordering of the rods. The histogram is also shown for the case of trivalent counterions in Fig. 5c. While the histogram is similar to the monovalent case in the large- $a$  regime and in the nematic phase, for intermediate values of  $a$  it develops a maximum at some angle that is characteristic of the clusters that form when the multivalent counterions link neighboring rods (see Fig. 2a).

The histogram of  $\cos \theta$  can be used to determine the average density profile of the rods. One can define the fluctuating density  $\rho_{\text{Rod}}(\mathbf{r}) = \frac{N_m}{L} \sum_i \int_0^L ds \delta^3(\mathbf{r} - \hat{\mathbf{t}}_i s)$  where  $\hat{\mathbf{t}}_i$  denotes the unit director of the  $i$ -th rod, and the rods are assumed to have a smeared charge distribution for simplicity of the presentation. We define the average density profile as  $n_{\text{Rod}}(z) = \frac{1}{N_r a^2} \int dx dy \langle \rho_{\text{Rod}}(\mathbf{r}) \rangle$ , where the averaging over the direction of the rods can be

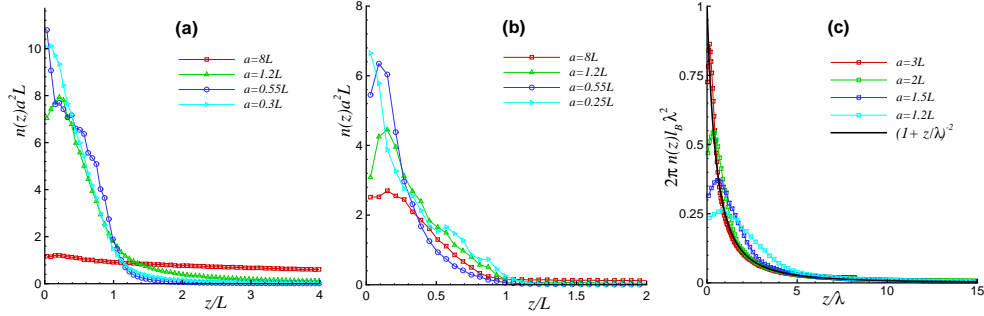


Fig. 6: The number density of counterions in units of  $a^{-2}L^{-1}$  as a function of  $z/L$  for different values of  $a$  for a)  $Z = 1$  and b)  $Z = 3$ . c) Rescaled number density of monovalent counterions as functions of  $z/\lambda$ .

performed using the distribution  $P(\cos\theta)$ . After some straightforward manipulation, one can write the density profile as  $n_{\text{Rod}}(z) = \frac{N_m}{La^2} \int_{z/L}^1 \frac{dt}{t} P(t)$ . This expression shows that the density profile of the rods will have a singular behavior near the surface if the  $\cos\theta = 0$  part of the distribution is nonzero, *i.e.* a non-vanishing fraction of the rods lie on surface.

We have also obtained the counterion density profile as a function of  $z$  for each value of  $a$ , as shown in Fig. 6a for  $Z = 1$ , and in Fig. 6b for  $Z = 3$ . For all values of the spacing, the general expectation that the counterions are confined within a distance of the order the Gouy-Chapman length holds true. This is demonstrated in Fig. 6c where the profiles are compared with the exact solution of the Poisson-Boltzmann equation for a flat uniformly charged surface  $n(z) = \frac{1}{2\pi Z^2 l_B \lambda^2} \frac{1}{(1+z/\lambda)^2}$ , with the Gouy-Chapman length being  $\lambda = \frac{a^2}{2\pi Z l_B N_m}$  as above. While for  $a \gg L$  the profiles follow the Poisson-Boltzmann solution, deviations appear for  $a \sim L$  presumably due to the condensation of the counterions inside the brush. It is interesting to note that all the profiles in Fig. 6c collapse on the Poisson-Boltzmann solution for  $z > 5\lambda$ . Although not attempted here, we note that more elaborate solutions of the Poisson-Boltzmann equation suited to the brush geometry can be used to account for the profiles obtained via simulation [20].

The counterion density profiles appear to develop a depletion in the vicinity of the surface for  $a > 0.55L$ , as can be seen in Figs. 6a and 6b. This feature is absent for  $a < 0.55L$ , presumably due to the emergence of the nematic ordering. In fact, one observes that the depletion is present so long as the  $\cos\theta = 0$  part of the histogram for the rods is non-vanishing. This suggests that the singular behavior of the density profile of the rods near the surface (described above) might cause the depletion of the counterions by way of excluded volume interaction: as long as some of the rods are lying on the surface, they jam the space near the surface and deplete the counterions. The range of the depletion in the profiles of Figs. 6a and 6b ( $\sim 2\sigma$ ) is consistent with this picture [21].

In conclusion, we have studied the collective behavior of rod-like polyelectrolytes that are end-grafted on a substrate, in the presence of mono- and trivalent counterions. We have demonstrated that the interplay between condensation of counterions and the repulsion of the rods can bring about a number of different regimes, while multivalent counterions can introduce correlations that lead to a structured collapse of the brush. The emergence of such patterns in the rod conformations—of staggered type for monovalent counterions and with “tepee frameworks” in case of the trivalent—seems to originate from similar free energy minimizing effects, and might have practical applications, in the design of DNA chips.

\* \* \*

It is a pleasure to acknowledge fruitful discussions with B. Bozorgui, M. Grubb, J.-F.

Joanny, R.R. Netz, D. Sackett, and J. Ulstrup.

REFERENCES

- [1] A.G. Moreira and R.R. Netz, in *Electrostatic Effects in Soft Matter and Biophysics*, edited by C. Holm, P. Kekicheff, and R. Podgornik (Kluwer, Boston, 2001); A.Yu. Grosberg, T.T. Nguyen, and B.I. Shklovskii, *Rev. Mod. Phys.* **74**, 329 (2002).
- [2] J. Widom and R.L. Baldwin, *Biopolymers* **22**, 1595 (1983); V.A. Bloomfield, *Biopolymers* **31**, 1471 (1991).
- [3] T.D. Pollard and J.A. Cooper, *Annu. Rev. Biochem.* **55**, 987 (1986); P.A. Jamney *et al.*, *Nature (London)* **345**, 89 (1990); G. Isenberg, *Semin. Cell Div. Biol.* **7**, 707 (1996).
- [4] G.C.L. Wong *et al.*, *Phys. Rev. Lett.* **91**, 018103 (2003).
- [5] K.-C. Lee *et al.*, *Phys. Rev. Lett.* **93**, 128101 (2004).
- [6] I. Borukhov, R.F. Bruinsma, *Phys. Rev. Lett.* **87**, 158101 (2001).
- [7] H. Fazli, R. Golestanian, and M. R. Kolahchi, *Phys. Rev. E* **72**, 011805 (2005).
- [8] For a recent review, see: J. R uhe *et al.*, *Adv. Polym. Sci.* **165**, 79 (2004).
- [9] M. V. Sataric and J. A. Tuszynski, *Phys. Rev. E* **67**, 011901 (2003).
- [10] Z. Wang and M.P. Sheetz, *Biophys J.* **78**, 1955 (2000).
- [11] D. J. Needleman *et al.*, *Phys. Rev. Lett.* **93**, 198104 (2004).
- [12] A. Halperin, A. Buhot, and E. B. Zhulina, *Biophys J.* **89**, 796 (2005).
- [13] H. Wackerbarth *et al.* *Angew. Chem. Int. Ed.* **43**, 198 (2004); *Langmuir* **20**, 1647 (2004).
- [14] P. Guenoun *et al.*, *Phys. Rev. Lett.* **81** 3872 (1998).
- [15] J. Lekner, *Physica A* **176**, 485 (1991).
- [16] M. Roger *et al.*, *Eur. Phys. J. E* **9**, 313 (2002).
- [17] G.S. Manning, *J. Chem. Phys.* **51**, 954 (1969); F. Oosawa, *Biopolymers* **6**, 134 (1968).
- [18] L. Onsager, *Ann. N.Y. Acad. Sci.* **51**, 627 (1949).
- [19] B.-Y. Ha and A.J. Liu, *Phys. Rev. Lett.* **79**, 1289 (1997); M. Kardar and R. Golestanian, *Rev. Mod. Phys.* **71**, 1233 (1999).
- [20] For a related study in the context of flexible polyelectrolyte brushes see: C.D. Santangelo and A.W.C. Lau, *Eur. Phys. J. E* **13**, 335 (2004).
- [21] S. Asakura and F. Oosawa, *J. Chem. Phys.* **22**, 1255 (1954).